

Research paper

Dynamics of a three-species food chain model with fear effect

Pingping Cong^a, Meng Fan^{a,*}, Xingfu Zou^b^aSchool of Mathematics and Statistics, Northeast Normal University, 5268 Renmin Street, Changchun, Jilin, 130024, P. R. China^bDepartment of Applied Mathematics, University of Western Ontario, London, ON, N6A 5B7, Canada

ARTICLE INFO

Article history:

Received 22 October 2020

Revised 3 February 2021

Accepted 9 March 2021

Available online 11 March 2021

Keywords:

Food chain model

Fear effect

Bistable phenomenon

Bifurcation

ABSTRACT

In this paper a three-species food chain model is formulated to investigate the impact of fear. First, we derive the predator's functional response by using the classical Holling's time budget argument and formulate a three-species food chain model where the cost and benefit of anti-predator behaviours are included. Then we study the dissipativity of the system and perform analysis on the existence and stability of equilibria. At last, we use numerical simulations to more visually explore the effects of fear on three species. The results show that the predator's fear effect can transform the system from chaotic dynamics to a stable state. Our results may provide some useful biological insights into ecosystems containing predator-prey interactions.

© 2021 Elsevier B.V. All rights reserved.

1. Introduction

In ecosystems, predator-prey interactions play a very important role, and understanding the mechanism that drives predator-prey system is a great challenge in ecology and evolutionary biology. It is well known that predation has been considered the major factor in interactions between predator and prey. A predator consumes a prey by hunting and killing it in nature. However, increasing evidences indicate that many animals also can assess the risk of predation, thereby changing their behaviours [19]. The fear of predator on prey, although not direct killing, still influences the population dynamics of both predator and prey. And there is evidence that this indirect effect can be as large as the direct effect [5,13,25,30,40]. Therefore, it is insufficient for us to consider only direct killing effect when studying the interactions between predator and prey [5].

As the prey becomes aware of the risk of predation, the prey may demonstrate certain types of anti-predator responses, such as changing its behaviours, its time of foraging and its reproduction [25,40]. Such responses will ultimately affect the population density of the prey. In terms of *foraging behaviour*, the prey may choose to stay in a safer place away from the high risk region to avoid being killed directly. In terms of *foraging time*, the prey species may also choose to reduce its foraging activities with some risk, forcing it to adopt a hungry survival mechanism, consequently, its growth rate will be reduced [26,30]. For example, in a recent experimental study on free-living mesocarnivore (raccoon) populations, by using month-long playbacks of large carnivore's vocalizations, Suraci et al. [30] showed that the foraging can be reduced due to the fear of predation risk, without direct killing. Altendorf et al. [1] predicted that mule deer would spend less time foraging and have the higher vigilance behavior when it is in fear of being predated by mountain lions.

In this context, several papers have shown that the presence of predators can cause significant reductions in some animal reproduction. Ylönen [37] reported that mustelid predators can inhibit the reproduction of bank voles, and an explana-

* Corresponding author:.

E-mail addresses: congpp882@nenu.edu.cn (P. Cong), mfan@nenu.edu.cn (M. Fan), xzou@uwo.ca (X. Zou).

tion was subsequently given that female’s behavior changed by the exposure to mustelid odours, which avoid copulations [27,38,39]. Creel et al. [4] also gave a similar conclusion: the reproductive cost of anti-predator behaviour may be high, which has an important impact on the dynamics of prey. Recent experiments have shown that the control of fear can be sufficient to affect ecosystem population dynamics, Zanette et al. [40] experimented throughout the sparrow’s entire breeding season, by eliminating direct killing and using predator’s voice playback to manipulate perceived risk. They observed that the reproduction rate of the song sparrows decreased by 40 percent due to the fear of predator alone. This suggests that perception of predation risk is sufficient to affect the reproduction of some animals.

Anti-predator behaviour of prey is ubiquitous, and the fear effect can be large, suggesting that the impact of fear on population dynamics cannot be ignored. With this motivation, Wang et al. [32] proposed a two-dimensional predator-prey model by incorporating the cost of fear into the growth of prey. Their results show the anti-predator response plays an important role on stabilizing the predator-prey system. They also observed that the Hopf bifurcation can occur and can be both supercritical and subcritical in the model incorporated with the cost of fear, which is different from previous classic predator-prey models. After this research, some different predator-prey systems incorporated with the fear effect have been proposed and analyzed, see, e.g., [3,6,8,14,15,21,23,24,28,29,31,33,34] and [35,36].

Among the above works, Panday et al. [23] proposed a three-species food chain model incorporated with the cost of fear into the reproduction of prey and middle predator, Panday et al. [24] also considered the cost of fear in foraging of the middle predator. In [36], motivated by the recent field experiment results in [30], the authors considered a food chain system consisting of four species; and depending on whether or not the top predator (large carnivore) is involved in predated the middle mesocarnivore, they proposed and analysed a 3-D ordinary system and a 4-D ordinary system respectively, with fear effect incorporated in the layer of mesocarnivore or/and large carnivore. The results on these systems all showed that the fear effect can make the biological systems behave differently, leading to very rich and complicated population dynamics.

As a long-term high level anti-predatory behaviour, it can lead to reduced production and foraging, there are both costs and benefits for the prey. The benefit of anti-predator behaviour mainly lies in reducing the predation, while the cost is that starvation affects its growth due to reduced predation, and hence the fear of predation affects reproduction of prey. In contrast, most analyses (if not all) of three-species food chain systems do not consider all costs and benefits of anti-predator behaviour.

In this paper, we will firstly revisit the functional responses in a three-species food chain system in the existence of fear effect. We will follow the classical Holling’s handling time argument to derive new functional responses, and then incorporate the newly derived functional responses into a classical three-species food chain system to obtain our model in Sect. 2. We consider the scenario that the fear of middle predator will reduce prey’s birth rate. Our proposed model can also describe the fear effect on animal foraging activity based on the detailed analysis of the underlying mechanisms of animal foraging behaviours that incorporate the costs and the benefits of anti-predator behaviour. In Sect. 3, we analyze the dissipativity of the model; in addition, we present some results on the existence and stability of equilibria. Some of our mathematical results are different from the classic models that ignore fear effects. We also perform some numerical simulations in Sect. 4 to demonstrate our results. We conclude the paper by Sect. 5 in which we present some discussions on the biological implications of our analytic results, together with some more detailed discussions on the consequences of fear effect.

2. Model formulation

In this section, we derive a mathematical model to describe the influence of fear effect on a three-species food chain system. Three ordinary differential equations are obtained below to describe the population dynamics of the prey, the middle predator or mesopredator which is also the prey of the top predator, and the top predator, with top-down cascade predation interactions. In the following modelling process, we will start from the classical three-species food chain system, and gradually introduce the fear effect of the middle predator on its prey and the fear effect of the top predator on the middle predator into the food chain system.

A classical three-species food chain system has the following general form

$$\begin{aligned} \frac{dx}{dt} &= bx - dx - ax^2 - g_1(x)y, \\ \frac{dy}{dt} &= e_1g_1(x)y - g_2(y)z - d_1y, \\ \frac{dz}{dt} &= e_2g_2(y)z - d_2z, \end{aligned} \tag{2.1}$$

where $x(t)$, $y(t)$, $z(t)$ are populations of the prey, the middle predator and the top predator at time t respectively, b is the birth rate of the prey, a is the intra-species competition coefficient of the prey, d , d_1 and d_2 are the natural mortality rates of the prey, the middle predator and the top predator respectively, e_1 and e_2 are the conversion efficiencies of middle predator and top predator respectively, $g_1(x)$ and $g_2(y)$ are the prey dependent functional responses of the middle predator and the top predator respectively.

From [32], the fear effect of the middle predator on the prey mainly affects the birth rate b of the prey. This is because the presence of the middle predator changes the reproductive habits and foraging behaviors of the prey. Considering the cost

of anti-predator defence of the prey, we assume that the modified birth rate of prey becomes $b/(1 + \alpha y)$. Here α reflects the level of fear which drives the anti-predator behaviours of the prey.

The fear effect of the top predator on the middle predator is mainly reflected in the feeding process of the middle predator, which prolongs the feeding time. This means that the functional response $g_1(x)$ of the middle predator should be related to the top predator. We next introduce this fear effect into $g_1(x)$ based on the classical Holling's time budget argument [12]. For more details on this method, please refer to the references [10] and [42].

Let T be the total time spent by a middle predator for gathering food from the prey. T is divided into three parts:

- (i) T_{ysx} is the time spent by the middle predator for searching the prey;
- (ii) T_{yhx} is the time spent by the middle predator for handling the caught prey;
- (iii) T_{yzw} is the time wasted by the middle predator, when it is interfered by the top predator due to the fear effect.

Here we do not consider the time wasted by the middle predator y for interfering with other middle predators y .

Let α_{ysx} be the searching efficiency of the middle predator for the prey and α_{yze} be the encounter rate between the middle predator and the top predator. We assume that

- (A1) the number of the prey caught by per middle predator is proportional to the prey density and the search time;
- (A2) the total time spent on handling the caught prey is equal to the product of the total number of the caught prey and the expected handling time t_{yhx} on each caught prey;
- (A3) the number of the top predator encountered by per middle predator is proportional to the top predator density and the search time;
- (A4) when a middle predator perceives/encounters a top predator, the intention of avoidance will cause a waste of time for the middle predator's search for its prey, we assume that the wasted time is the same for all middle predators, and denote it by t_{yzw} .

It follows from (A1) and (A2) that the total number of the prey caught by per middle predator is $N_{yx} = \alpha_{ysx}xT_{ysx}$. Then

$$T_{yhx} = N_{yx}t_{yhx} = \alpha_{ysx}t_{yhx}xT_{ysx}. \tag{2.2}$$

From (A3) and (A4), we conclude that the number of the top predator encountered by per middle predator is $N_{yz} = \alpha_{yze}zT_{ysx}$. Hence

$$T_{yzw} = N_{yz}t_{yzw} = \alpha_{yze}t_{yzw}zT_{ysx}. \tag{2.3}$$

Combining (i)-(iii) with (2.2), (2.3) gives

$$T = T_{ysx} + T_{yhx} + T_{yzw} = T_{ysx} + \alpha_{ysx}t_{yhx}xT_{ysx} + \alpha_{yze}t_{yzw}zT_{ysx}.$$

Therefore, the functional response of the middle predator reads

$$g_1(x, z) := \frac{N_{yx}}{T} = \frac{\alpha_{ysx}x}{1 + \alpha_{ysx}t_{yhx}x + \alpha_{yze}t_{yzw}z}. \tag{2.4}$$

The classical functional response $g_1(x)$ for the predation of y on x now becomes $g_1(x, z)$, which depends not only on x but also on z (the predator of species y). Let the functional response of the top predator (z) be of Holling type II, that is,

$$g_2(y) = \frac{\gamma\alpha_{zsy}y}{1 + \gamma\alpha_{zsy}t_{zhy}y}, \tag{2.5}$$

where α_{zsy} is the searching efficiency of the top predator for the middle, $1 - \gamma \in [0, 1)$ is the reduced searching efficiency due to the vigilance arising from fear of species z on y and t_{zhy} is the expected handling time needed for an individual in species z on each caught y individual.

Combining all (2.1), (2.4) and (2.5), we have the following three-species food chain model with fear effect

$$\begin{aligned} \frac{dx}{dt} &= \frac{bx}{1 + \alpha y} - dx - ax^2 - \frac{\alpha_{ysx}xy}{1 + \alpha_{ysx}t_{yhx}x + \alpha_{yze}t_{yzw}z}, \\ \frac{dy}{dt} &= \frac{e_1\alpha_{ysx}xy}{1 + \alpha_{ysx}t_{yhx}x + \alpha_{yze}t_{yzw}z} - \frac{\gamma\alpha_{zsy}yz}{1 + \gamma\alpha_{zsy}t_{zhy}y} - d_1y, \\ \frac{dz}{dt} &= \frac{e_2\gamma\alpha_{zsy}yz}{1 + \gamma\alpha_{zsy}t_{zhy}y} - d_2z. \end{aligned} \tag{2.6}$$

For the convenience of the following discussion, rescaling the parameters by

$$a_1 = \alpha_{ysx}, \quad a_2 = \gamma\alpha_{zsy}, \quad h_1 = t_{yhx}, \quad h_2 = t_{zhy}, \quad \beta = \alpha_{yze}t_{yzw}.$$

Then the model (2.6) becomes

$$\frac{dx}{dt} = \frac{bx}{1 + \alpha y} - dx - ax^2 - \frac{a_1xy}{1 + a_1h_1x + \beta z} \equiv xf_1(x, y, z),$$

$$\begin{aligned} \frac{dy}{dt} &= \frac{e_1 a_1 xy}{1 + a_1 h_1 x + \beta z} - \frac{a_2 yz}{1 + a_2 h_2 y} - d_1 y \equiv y f_2(x, y, z), \\ \frac{dz}{dt} &= \frac{e_2 a_2 yz}{1 + a_2 h_2 y} - d_2 z \equiv z f_3(x, y, z). \end{aligned} \tag{2.7}$$

In (2.7), for the bottom species x , as in [32], we only assume that the fear of species y on species x will cause a decline in production rate reflected by the reducing function $1/(1 + \alpha y)$ with the parameter accounting for the fear level by species x . The top predator z , its predation on y is presented by nothing but a Holling Type II or Michaelis-Menten functional response. For the middle species y , its predation on x is given by the functional response of $a_1 x / (1 + a_1 h_1 x + \beta z)$; it also reduces to the Holling Type II functional response when $\beta = 0$, which accounts for the scenario that foraging for and predation on the prey x by middle predator y is not interfered (no fear) by the top predator z . However, when $\beta > 0$, the predation rate is changed from $a_1 x / (1 + a_1 h_1 x)$ to $a_1 x / (1 + a_1 h_1 x + \beta z)$, and thus, β is such a parameter that represents the level of the fear that species y may perceive and respond to. In addition to the effect on its foraging for species x reflected by $\beta > 0$, the fear of species z on y species activates a vigilance which will make the species z 's searching for y more difficult, and thus, the parameter $a_2 = \gamma \alpha_{zsy}$ (assuming $a_2 < 1$) also explains another effect of the fear for species y . In summary, the rescaled model (2.7) contains three parameters (α , β , and a_2) that are related to the fear effects of the two preys (bottom prey x and meso-prey y) in different aspects in the three-species food chain ecological system. This is in contrast to the existing models mentioned above where generally only one fear parameter is incorporated, and hence, the effects at different levels and in different aspects cannot be separated.

Considering the biological background of (2.7), we will assume that all the parameters in (2.7) are positive unless explicitly stated otherwise, and will consider the solutions of (2.7) with nonnegative initial value, i.e., $x(0), y(0), z(0) \geq 0$.

3. Mathematical analysis

In this section, we first investigate some basic dynamical properties of system (2.7), furthermore, we investigate the existence and stability of equilibria.

Lemma 3.1. \mathbb{R}_+^3 is a positive invariant set of system (2.7). Moreover,

$$\Delta = \left\{ (x, y, z) \in \mathbb{R}_+^3 \mid x + \frac{y}{e_1} + \frac{z}{e_1 e_2} \leq \frac{(b - d + \mu)^2}{4a\mu} \right\}$$

is a globally attracting region, which implies that system (2.7) is dissipative.

Proof. It follows from (2.7) that

$$\begin{aligned} x(t) &= x(0) \exp \left(\int_0^t f_1(x(s), y(s), z(s)) ds \right), \\ y(t) &= y(0) \exp \left(\int_0^t f_2(x(s), y(s), z(s)) ds \right), \\ z(t) &= z(0) \exp \left(\int_0^t f_3(x(s), y(s), z(s)) ds \right), \end{aligned}$$

which implies that solutions with initial condition in \mathbb{R}_+^3 remain there for all forward times.

Let

$$P(t) = x(t) + \frac{1}{e_1} y(t) + \frac{1}{e_1 e_2} z(t)$$

and $\mu = \min\{d_1, d_2\}$. A direct calculation gives

$$\begin{aligned} \frac{dP}{dt} &\leq x(b - d - ax) - \frac{d_1}{e_1} y - \frac{d_2}{e_1 e_2} z \\ &\leq x(b - d - ax + \mu) - \mu \left(x + \frac{1}{e_1} y + \frac{1}{e_1 e_2} z \right), \end{aligned}$$

hence

$$\begin{aligned} \frac{dP}{dt} + \mu P &\leq x(b - d - ax + \mu) \\ &= -a \left(x - \frac{b - d + \mu}{2a} \right)^2 + \frac{(b - d + \mu)^2}{4a} \leq \frac{(b - d + \mu)^2}{4a}. \end{aligned}$$

This means that

$$P(t) \leq \frac{(b - d + \mu)^2}{4a\mu} (1 - e^{-\mu t}) + P(0)e^{-\mu t},$$

and

$$\limsup_{t \rightarrow \infty} P(t) = \frac{(b - d + \mu)^2}{4a\mu}.$$

Therefore, the conclusion of the lemma holds. \square

Next, we investigate the existence and stability of equilibria. The possible equilibria or steady states of system (2.7) are listed below:

$$E_0 : (0, 0, 0), \quad E_1 : \left(\frac{b-d}{a}, 0, 0 \right),$$

$E_2 : (x_2, y_2, 0)$, where (x_2, y_2) satisfies

$$\frac{b}{1 + \alpha y} - d - ax - \frac{a_1 y}{1 + a_1 h_1 x} = 0, \quad \frac{e_1 a_1 x}{1 + a_1 h_1 x} - d_1 = 0, \tag{3.1}$$

$E_3 : (x_3, y_3, z_3)$, where (x_3, y_3, z_3) satisfies

$$\begin{aligned} \frac{b}{1 + \alpha y} - d - ax - \frac{a_1 y}{1 + a_1 h_1 x + \beta z} &= 0, \\ \frac{e_1 a_1 x}{1 + a_1 h_1 x + \beta z} - \frac{a_2 z}{1 + a_2 h_2 y} - d_1 &= 0, \\ \frac{e_2 a_2 y}{1 + a_2 h_2 y} - d_2 &= 0. \end{aligned} \tag{3.2}$$

In order to obtain the local stability of these equilibria, we first calculate the Jacobian matrix as

$$J(x, y, z) = \begin{pmatrix} a_{11} & a_{12} & a_{13} \\ a_{21} & a_{22} & a_{23} \\ a_{31} & a_{32} & a_{33} \end{pmatrix}, \tag{3.3}$$

where

$$\begin{aligned} a_{11} &= \frac{b}{1 + \alpha y} - d - 2ax - \frac{a_1 y(1 + \beta z)}{(1 + a_1 h_1 x + \beta z)^2}, \\ a_{12} &= -\frac{\alpha b x}{(1 + \alpha y)^2} - \frac{a_1 x}{1 + a_1 h_1 x + \beta z}, \quad a_{13} = \frac{\beta a_1 x y}{(1 + a_1 h_1 x + \beta z)^2}, \\ a_{21} &= \frac{e_1 a_1 y(1 + \beta z)}{(1 + a_1 h_1 x + \beta z)^2}, \quad a_{22} = \frac{e_1 a_1 x}{1 + a_1 h_1 x + \beta z} - \frac{a_2 z}{(1 + a_2 h_2 y)^2} - d_1, \\ a_{23} &= -\frac{\beta e_1 a_1 x y}{(1 + a_1 h_1 x + \beta z)^2} - \frac{a_2 y}{1 + a_2 h_2 y}, \quad a_{31} = 0, \quad a_{32} = \frac{e_2 a_2 z}{(1 + a_2 h_2 y)^2}, \\ a_{33} &= \frac{e_2 a_2 y}{1 + a_2 h_2 y} - d_2. \end{aligned}$$

Theorem 3.1. *If $b < d$, then E_0 is globally asymptotically stable; if $b > d$, then E_0 is unstable.*

Proof. From (3.3), we have

$$J(E_0) = \begin{pmatrix} b-d & 0 & 0 \\ 0 & -d_1 & 0 \\ 0 & 0 & -d_2 \end{pmatrix},$$

which implies that E_0 is locally asymptotically stable if $b < d$, and if $b > d$, then E_0 is unstable. Note that if $b < d$ holds, then

$$\begin{aligned} \frac{dx}{dt} &= \frac{bx}{1 + \alpha y} - dx - ax^2 - \frac{a_1 xy}{1 + a_1 h_1 x + \beta z} \\ &\leq (b-d)x - ax^2 - \frac{a_1 xy}{1 + a_1 h_1 x + \beta z} < 0. \end{aligned} \tag{3.4}$$

It is easy to see when $b < d$, $x(t)$ goes to zero as $t \rightarrow \infty$ by simple comparison, which triggers $y(t)$ and $z(t)$ going to zero as well (this is also quite natural from biological meaning). Hence E_0 is globally attractive, implying that E_0 is indeed globally asymptotically stable. \square

Theorem 3.2. *Assume that $b > d$, then E_1 exists. Moreover, E_1 is globally asymptotically stable if*

$$\frac{e_1 a_1 (b-d)}{a + a_1 h_1 (b-d)} < d_1. \tag{3.5}$$

Proof. It follows from (3.3) that

$$J(E_1) = \begin{pmatrix} d-b & \frac{a_1(d-b)}{a+a_1h_1(b-d)} + \frac{\alpha b(d-b)}{a} & 0 \\ 0 & \frac{e_1a_1(b-d)}{a+a_1h_1(b-d)} - d_1 & 0 \\ 0 & 0 & -d_2 \end{pmatrix},$$

which means that E_1 is locally asymptotically stable if $b > d$ and (3.5) holds.

From (2.7), we have

$$\begin{aligned} \frac{dy}{dt} &= \frac{e_1a_1xy}{1+a_1h_1x+\beta z} - \frac{a_2yz}{1+a_2h_2y} - d_1y \\ &< \left(\frac{e_1a_1(b-d)}{a+a_1h_1(b-d)} - d_1 \right) y. \end{aligned}$$

According to the comparison theorem, $y(t) \rightarrow 0$ as $t \rightarrow \infty$ if (3.5) holds. Furthermore, we also have $z(t) \rightarrow 0$ as $y(t) \rightarrow 0$. From the theory of asymptotical autonomous systems [20], (2.7) reduces to a limiting system

$$\frac{dx}{dt} = bx - dx - ax^2, \tag{3.6}$$

which implies that $x(t) \rightarrow (b-d)/a$. This means that E_1 is globally attractive. Therefore E_1 is globally asymptotically stable. \square

Note that E_2 is obtained by solving (3.1). A simple calculation gives

$$\begin{aligned} x_2 &= \frac{d_1}{e_1a_1 - a_1h_1d_1}, \\ y_2 &= \frac{-a_1 - \alpha m + \sqrt{(a_1 + \alpha m)^2 + 4a_1\alpha(b-d - ax_2)(1 + a_1h_1x_2)}}{2a_1\alpha}, \end{aligned} \tag{3.7}$$

where $m = (d + ax_2)(1 + a_1h_1x_2)$.

Theorem 3.3. Assume that

$$d < b, \quad d_1 < \frac{(b-d)e_1a_1}{a+(b-d)a_1h_1},$$

then E_2 exists. Moreover,

(i) if

$$a > \frac{a_1^2h_1y_2}{(1+a_1h_1x_2)^2} \quad \text{and} \quad d_2 > \frac{e_2a_2y_2}{1+a_2h_2y_2}, \tag{3.8}$$

then E_2 is locally asymptotically stable;

(ii) if

$$d_2 > \frac{e_2}{h_2} \quad \text{and} \quad d_1 \geq \max \left\{ \frac{e_1 - bh_1}{h_1}, \frac{e_1((b-d)a_1h_1 - a)}{h_1(a + a_1h_1(b-d))} \right\}, \tag{3.9}$$

then E_2 is globally asymptotically stable.

Proof. The existence of E_2 is obvious. It follows from (3.3) that the local stability of E_2 is determined by

$$J(E_2) = \begin{pmatrix} a_{11} & a_{12} & a_{13} \\ a_{21} & 0 & a_{23} \\ 0 & 0 & a_{33} \end{pmatrix},$$

where

$$\begin{aligned} a_{11} &= \frac{a_1^2h_1x_2y_2}{(1+a_1h_1x_2)^2} - ax_2, & a_{12} &= -\frac{\alpha bx_2}{(1+\alpha y_2)^2} - \frac{a_1x_2}{1+a_1h_1x_2}, \\ a_{13} &= \frac{\beta a_1x_2y_2}{(1+a_1h_1x_2)^2}, & a_{21} &= \frac{e_1a_1y_2}{(1+a_1h_1x_2)^2}, \\ a_{23} &= -\frac{\beta d_1y_2}{1+a_1h_1x_2} - \frac{a_2y_2}{1+a_2h_2y_2}, & a_{33} &= \frac{e_2a_2y_2}{1+a_2h_2y_2} - d_2. \end{aligned}$$

If (3.8) holds, then

$$a_{11} < 0, \quad a_{12}a_{21} < 0, \quad a_{33} < 0,$$

which imply that all three eigenvalues of the characteristic equation of $J(E_2)$ have negative real parts, confirming the locally asymptotic stability of E_2 . Therefore, (i) holds.

Note that if $d_2 > e_2/h_2$, then

$$\frac{dz}{dt} = \frac{e_2 a_2 y z}{1 + a_2 h_2 y} - d_2 z < \left(\frac{e_2}{h_2} - d_2\right) z,$$

which implies that $z(t) \rightarrow 0$ as $t \rightarrow \infty$. Thus, (2.7) reduces to a limiting system

$$\begin{cases} \frac{dx}{dt} = \frac{bx}{1 + \alpha y} - dx - ax^2 - \frac{a_1 xy}{1 + a_1 h_1 x}, \\ \frac{dy}{dt} = \frac{e_1 a_1 xy}{1 + a_1 h_1 x} - d_1 y. \end{cases} \tag{3.10}$$

By the results in [32], (x_2, y_2) is globally asymptotically stable for (3.10) if (3.9) holds. From the theory of asymptotically autonomous systems [20], (ii) holds. \square

We now investigate the existence and stability of E_3 . It follows from (3.2) that

$$y_3 = \frac{d_2}{e_2 a_2 - d_2 a_2 h_2}, \quad z_3 = \frac{a_1 y_3 / (q - a x_3) - (1 + a_1 h_1 x_3)}{\beta}, \tag{3.11}$$

where $q = b / (1 + \alpha y_3) - d$. In order to explore the biologically meaningful existence of the equilibrium E_3 , we let

$$\begin{aligned} A_1 &= -2aq - \frac{d_2 a a_1 h_1}{e_1 e_2 \beta}, \quad A_2 = q^2 + \frac{e_2 \beta a d_1 y_3 + d_2 q a_1 h_1 - a d_2}{e_1 e_2 \beta}, \\ A_3 &= \frac{d_2 q - d_2 a_1 y_3 - d_1 y_3 q e_2 \beta}{e_1 e_2 \beta}. \end{aligned}$$

Then we have

$$\frac{bx}{1 + \alpha y} - dx - ax^2 - \frac{d_1}{e_1} y - \frac{d_2}{e_1 e_2} z = 0, \tag{3.12}$$

with x_3 satisfying

$$f(x) := a^2 x^3 + A_1 x^2 + A_2 x + A_3 = 0. \tag{3.13}$$

It is clear that

$$A_1 < 0, \quad f'(x) = a^2 x^2 + A_1 x + A_2.$$

From (3.11), if $x_3 > 0, z_3 > 0$, then $x_3 < q/a$. Next we use the Descartes sign rule to explore the number of positive root(s) of (3.13) in $(0, q/a)$.

Lemma 3.2. *In the interval $(0, q/a)$, the following conclusions hold.*

- (i) when $A_3 > 0$, (3.13) has a positive root;
- (ii) when $A_3 < 0$ and $A_2 < 0$, (3.13) has no positive root;
- (iii) when $A_3 < 0$ and $A_2 > 0$,
 - (iii-a) if one of the following conditions is true, then (3.13) has no positive root.
 - $\Delta < 0$ and $x^* > q/a$;
 - $\Delta > 0$;
 - $\Delta = 0$ and $A = 0$;
 - $\Delta = 0, A \neq 0$ and $x^* > q/a$;
 - (iii-b) if one of the following conditions is true, then (3.13) has two positive roots.
 - $\Delta < 0$ and $x^* < q/a$;
 - $\Delta = 0, A \neq 0$ and $x^* < q/a$;

where

$$\Delta = (A_1 A_2 - 9a^2 A_3)^2 - 4(A_1^2 - 3a^2 A_2)(A_2^2 - 3A_1 A_3), \quad x^* = -\frac{A_1 + \sqrt{A_1^2 - 3a^2 A_2}}{3a^2}. \tag{3.14}$$

Proof. (i) When $A_3 > 0$, the number of sign changes of adjacent non-zero coefficients in $f(x)$ is two. According to the Descartes sign rule, (3.13) has two positive roots or no positive root. Note that

$$f(q/a) = -\frac{d_2 a_1 y_3}{e_1 e_2 \beta} < 0. \tag{3.15}$$

Thus (3.13) has a positive root in $(0, q/a)$ (see Fig. 1(a)).

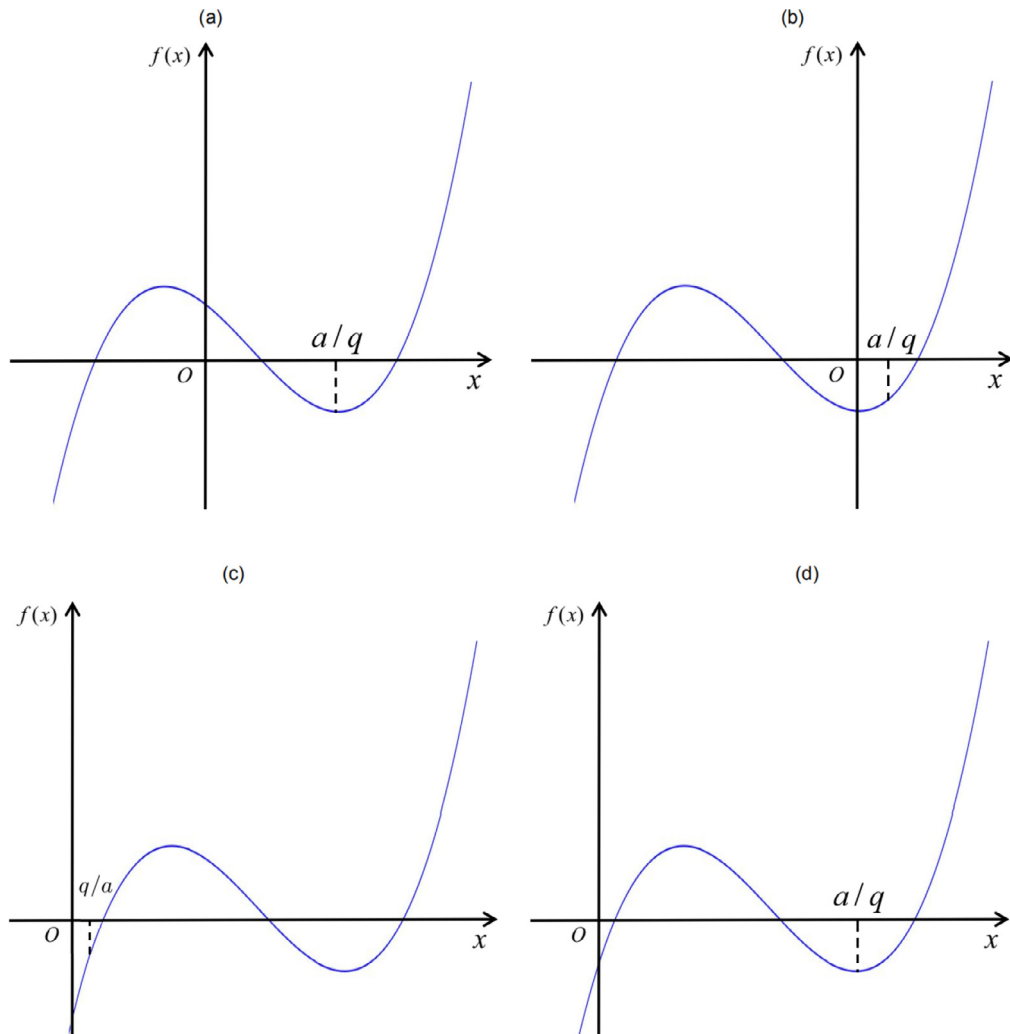


Fig. 1. The graph of the unary cubic equation (3.13) corresponding to the cases (i), (ii), (iii-a) and (iii-b). (a) The sign of adjacent non-zero coefficients in the unary cubic equation (3.13) changes twice and $f(a/q) < 0$, so (3.13) has two positive roots. (b) The number of sign changes in $f(x)$ is only one, (3.13) has one positive root. When the number of sign changes in $f(x)$ is three and (3.13) has three positive roots, (c) $x^* > q/a$, (d) $x^* < q/a$.

(ii) When $A_3 < 0$ and $A_2 < 0$, the number of sign changes of adjacent non-zero coefficients in $f(x)$ is only one. From Descartes sign rule, (3.13) has a unique positive root. But (3.15) holds, this means that in this case the equation has no positive root in $(0, q/a)$ (see Fig. 1(b)).

(iii) When $A_3 < 0$ and $A_2 > 0$, the number of sign changes of adjacent non-zero coefficients in $f(x)$ is three, (3.13) has one or three positive roots. Then from [11] we get the following cases.

(1) If $\Delta < 0$, then (3.13) has three unequal real roots. It follows that x^* is the smaller root of $f'(x) = 0$. From (3.15) and $x^* > q/a$, the equation has no positive root in $(0, q/a)$ (see Fig. 1(c));

(2) If $\Delta < 0$ and $x^* < q/a$, then (3.13) has two positive roots in $(0, q/a)$ (see Fig. 1(d));

(3) If $\Delta > 0$, then (3.13) has a unique real root, but it is outside $(0, q/a)$. Hence the equation has no positive root in $(0, q/a)$;

(4) If $\Delta = 0$ and $A = 0$, then (3.13) has three equal real roots, thus the equation has no positive root in $(0, q/a)$;

(5) If $\Delta = 0$ and $A \neq 0$, then (3.13) has three real roots where two real roots are equal. When $x^* > q/a$, the equation has no positive root in $(0, q/a)$. When $x^* < q/a$, (3.13) has two equal positive roots in $(0, q/a)$. \square

Lemma 3.2 gives conditions on the existence of x_3 in the interval $(0, q/a)$, therefore, the following existence theorem about E_3 can be obtained from Lemma 3.2.

Theorem 3.4. If (i) or (iii-b) in Lemma 3.2 holds and

$$d_2 < \frac{e_2}{h_2}, \quad 1 < \frac{a_1 y_3}{(q - ax_3)(1 + a_1 h_1 x_3)} \tag{3.16}$$

holds, then E_3 exists.

Remark 3.1. Note that while the first inequality in (3.16) is explicit, the second is implicit because it is expressed in terms of x_3 and y_3 , not directly in terms of the model parameters. However, once the model parameters are given, the coefficients of (3.13) can be directly calculated, and then x_3 can be obtained from (3.13) by the new extracting formula (Shengjin's formula) in [11] and y_3 can be calculated by (3.11), thereby verifying whether (3.16) holds or not.

We next explore the stability of E_3 . The Jacobian matrix at E_3 takes the form of

$$J(E_3) = \begin{pmatrix} a_{11} & a_{12} & a_{13} \\ a_{21} & a_{22} & a_{23} \\ 0 & a_{32} & 0 \end{pmatrix},$$

where

$$\begin{aligned} a_{11} &= \frac{a_1^2 h_1 x_3 y_3}{(1 + a_1 h_1 x_3 + \beta z_3)^2} - \alpha x_3, & a_{12} &= -\frac{\alpha b x_3}{(1 + \alpha y_3)^2} - \frac{a_1 x_3}{1 + a_1 h_1 x_3 + \beta z_3}, \\ a_{13} &= \frac{\beta a_1 x_3 y_3}{(1 + a_1 h_1 x_3 + \beta z_3)^2}, & a_{21} &= \frac{e_1 a_1 y_3 (1 + \beta z_3)}{(1 + a_1 h_1 x_3 + \beta z_3)^2}, & a_{22} &= \frac{a_2^2 h_2 y_3 z_3}{(1 + a_2 h_2 y_3)^2}, \\ a_{23} &= -\frac{\beta e_1 a_1 x_3 y_3}{(1 + a_1 h_1 x_3 + \beta z_3)^2} - \frac{d_2}{e_2}, & a_{32} &= \frac{e_2 a_2 z_3}{(1 + a_2 h_2 y_3)^2}. \end{aligned}$$

The characteristic equation of the Jacobian matrix is

$$\lambda^3 + c_1 \lambda^2 + c_2 \lambda + c_3 = 0,$$

where

$$c_1 = -(a_{11} + a_{22}), \quad c_2 = a_{11} a_{22} - a_{12} a_{21} - a_{23} a_{32}, \quad c_3 = -a_{32} (a_{13} a_{21} - a_{11} a_{23}).$$

In the following, we consider the case that there exists only one positive equilibrium point.

Theorem 3.5. Assume that E_3 exists. Then

- (i) if $c_1 > 0, 0 < c_3 < c_1 c_2$, then E_3 is locally asymptotically stable;
- (ii) if

$$\begin{aligned} \frac{(b-d-p+\alpha x_3)^2}{4a} + dx_3 + \frac{d_1 y_3}{e_1} + \frac{d_2 z_3}{e_1 e_2} < \frac{b x_3}{1 + \alpha Q}, \\ e_1 a_1 x_3 - \frac{a_2 z_3}{1 + a_2 h_2 Q} < d_1, \quad e_2 a_2 y_3 < d_2 \end{aligned} \tag{3.17}$$

holds, then $E_3 = (x_3, y_3, z_3)$ is globally asymptotically stable, where

$$Q = \frac{(b-d+\mu)^2}{4a\mu}, \quad \mu = \min\{d_1, d_2\}, \quad p = \frac{a_1 y_3}{1 + a_1 h_1 Q + \beta Q}. \tag{3.18}$$

Proof. (i) follows directly from the Routh-Hurwitz criteria. For (ii), we consider the Lyapunov function defined by

$$V = \left(x - x_3 - x_3 \ln \frac{x}{x_3}\right) + \frac{1}{e_1} \left(y - y_3 - y_3 \ln \frac{y}{y_3}\right) + \frac{1}{e_1 e_2} \left(z - z_3 - z_3 \ln \frac{z}{z_3}\right).$$

Differentiating V with respect to t , we have

$$\frac{dV(x(t), y(t), z(t))}{dt} = \left(1 - \frac{x_3}{x}\right) \frac{dx}{dt} + \frac{1}{e_1} \left(1 - \frac{y_3}{y}\right) \frac{dy}{dt} + \frac{1}{e_1 e_2} \left(1 - \frac{z_3}{z}\right) \frac{dz}{dt}.$$

According to the Lemma 3.1, since $0 < e_1, e_2 \leq 1$, there exists a T such that when $t > T$, $x(t), y(t), z(t) < Q$ and

$$\begin{aligned} \frac{dV}{dt} &\leq bx - dx - \alpha x^2 - \frac{b x_3}{1 + \alpha Q} + dx_3 + \alpha x_3 x + a_1 x_3 y - \frac{d_1 (y - y_3)}{e_1} - px + \frac{a_2 y_3 z}{e_1} \\ &\quad - \frac{d_2 (z - z_3)}{e_1 e_2} - \frac{a_2 z_3 y}{e_1 (1 + a_2 h_2 Q)} \\ &\leq -a \left(x - \frac{b-d-p+\alpha x_3}{2a}\right)^2 + \frac{(b-d-p+\alpha x_3)^2}{4a} - \frac{b x_3}{1 + \alpha Q} + dx_3 + \frac{d_1 y_3}{e_1} \\ &\quad + \frac{d_2 z_3}{e_1 e_2} + \left(a_1 x_3 - \frac{d_1}{e_1} - \frac{a_2 z_3}{e_1 (1 + a_2 h_2 Q)}\right) y + \left(\frac{a_2 y_3}{e_1} - \frac{d_2}{e_1 e_2}\right) z, \end{aligned}$$

where $Q = (b-d+\mu)^2/4a\mu$, $\mu = \min\{d_1, d_2\}$ and $p = a_1 y_3 / (1 + a_1 h_1 Q + \beta Q)$. It is observed that if

$$\frac{(b-d-p+\alpha x_3)^2}{4a} + dx_3 + \frac{d_1 y_3}{e_1} + \frac{d_2 z_3}{e_1 e_2} < \frac{b x_3}{1 + \alpha Q},$$

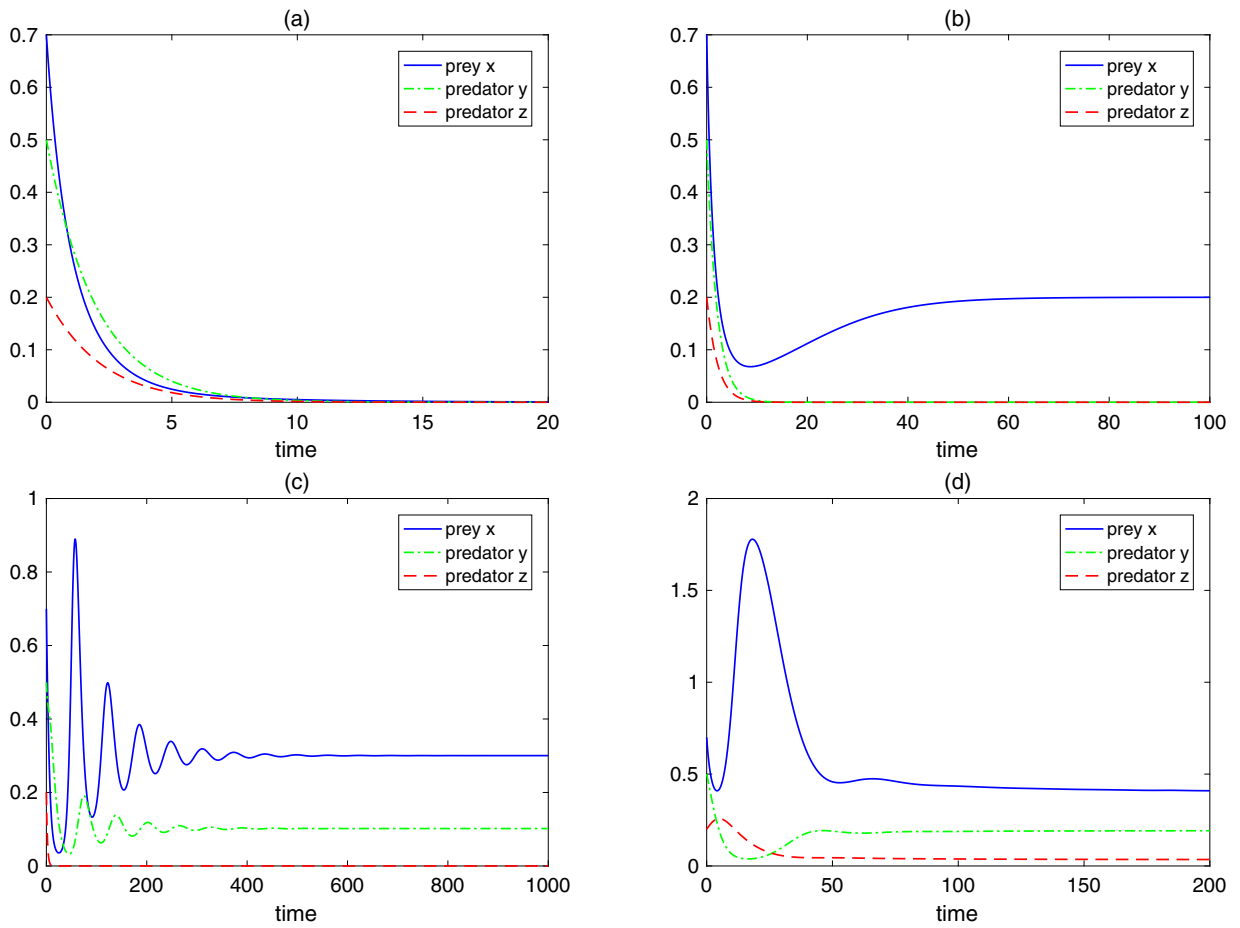


Fig. 2. Illustration of convergence to equilibrium dynamics of system (2.7) with initial value (0.7, 0.5, 0.2). The parameter values are given in Table 1 for (a), (b), (c) and (d) respectively, and they satisfy the conditions in Theorems 3.1, 3.2, 3.3 and 3.4 respectively, and hence, supporting the dynamics of convergence to the equilibria E_0, E_1, E_2 and E_3 , respectively. They demonstrate four different scenarios: (a) x cannot survive and accordingly, neither can y and z ; (b) x can survive but y and z cannot; (c) x and y can survive but z cannot; (d) all three species can survive.

$$e_1 a_1 x_3 < d_1 + \frac{a_2 z_3}{1 + a_2 h_2 Q}, \quad e_2 a_2 y_3 < d_2$$

holds, then $dV(\cdot)/dt \leq 0$, $dV(\cdot)/dt = 0$ if and only if $(x, y, z) \equiv (x_3, y_3, z_3)$. Consequently, by Lyapunov-Lasalle's invariance principle [18], the interior equilibrium $E_3(x_3, y_3, z_3)$ is globally asymptotically stable if (3.17) holds. \square

In the above, we have discussed the conditions of the existence and stability of all equilibria. All these analytical results can be numerically confirmed. For a demonstration, we present some simulation results in Fig. 2, that illustrate the dynamics of convergence to equilibria. In Fig. 2(a), the parameters are chosen (see Table 1) such that the growth rate of the bottom prey x is sufficiently small ($b < d$, the scenario of Theorem 3.1), and thus, as predicted by Theorem 3.1, all three species go to extinction. Similarly, Fig. 2(b), Fig. 2(c), and Fig. 2(d) corresponding to the scenarios of Theorems 3.2, 3.3, and 3.4 that demonstrate the convergence to equilibria E_1, E_2 , and E_3 respectively, with the parameters given in Table 1.

In addition to the aforementioned dynamics of global convergence to an equilibrium obtained in Theorems 3.1–3.4, we have also numerically observed periodic dynamics and bistable dynamics by choosing parameters that violate those conditions for global convergence to an equilibrium. See Fig. 3 for cyclic dynamics and Fig. 4 for bistable dynamics for system (2.7).

4. Impact of the fear effects

This section is devoted to some discussions on the role of the fear effect on the dynamics of the model. Note that, species x and y , as the prey of y and z respectively, each has an anti-predation response when perceiving a risk from its predator (y and z respectively). The response of x in this model is to reduce its production, with the level reflected by the parameter $\alpha > 0$. The response of the species y , however, are two-fold: (1) the vigilance of species y makes the species z 's

Table 1
Parameter values for attractors of (2.7) presented in Fig. 2.

Figures	Parameters	Attractors
Fig. 2(a)	$b = 0.5, d = 0.7, d_1 = 0.5, d_2 = 0.5, \alpha = 21.2, \beta = 20.7, a = 0.5, h_1 = 3, a_1 = 0.37, e_1 = 0.6, a_2 = 0.25, h_2 = 4, e_2 = 0.6$	E_0 is an attractor, the condition of total extinction in the system
Fig. 2(b)	$b = 0.5, d = 0.4, d_1 = 0.5, d_2 = 0.5, \alpha = 21.2, \beta = 20.7, a = 0.5, h_1 = 3, a_1 = 0.37, e_1 = 0.6, a_2 = 0.25, h_2 = 4, e_2 = 0.6$	E_1 is an attractor, where the middle predator and the top predator become extinct
Fig. 2(c)	$b = 0.5, d = 0.1, d_1 = 0.1, d_2 = 0.5, \alpha = 21.2, \beta = 20.7, a = 0.1, h_1 = 3, a_1 = 0.37, e_1 = 0.9, a_2 = 0.1, h_2 = 4, e_2 = 0.6$	E_2 is an attractor, where the prey and the middle predator can coexist at the equilibrium
Fig. 2(d)	$b = 1.3, d = 0.1, d_1 = 0.1, d_2 = 0.1, \alpha = 15, \beta = 23, a = 0.4, h_1 = 1, a_1 = 0.8, e_1 = 0.8, a_2 = 0.8, h_2 = 1.5, e_2 = 0.8$	All species coexist. E_3 is an attractor, the solution of (2.7) tends to a steady state

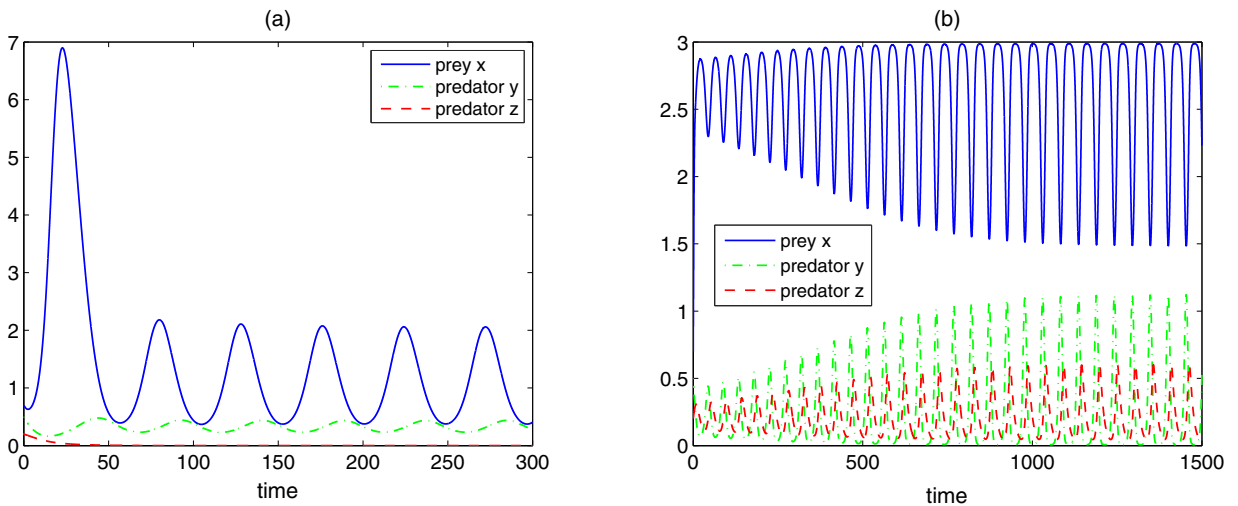


Fig. 3. Some cyclic dynamics of the system (2.7). Solutions starting at (0.7, 0.5, 0.2). (a) The top predator z is extinct while the prey x , the middle predator y coexist cyclically ($b = 1.2, d = 0.5, d_1 = 0.1, d_2 = 0.1, \alpha = 3.2, \beta = 26.4, a = 0.03, a_1 = 0.37, h_1 = 3, e_1 = 0.6, a_2 = 0.25, h_2 = 4, e_2 = 0.6$). (b) The prey, the middle predator and the top predator coexist cyclically ($b = 1.3, d = 0.1, d_1 = 0.1, d_2 = 0.1, \alpha = 0.5, \beta = 23, a = 0.4, a_1 = 0.8, h_1 = 1, e_1 = 0.8, a_2 = 0.8, h_2 = 1.5, e_2 = 0.8$).

predation on y more difficult and this effect is reflected by the parameter $a_2 = \gamma\alpha_{zsy}$; (II) the vigilance of species y also affects its own foraging effort for its prey x and this is measured by the parameter $\beta = \alpha_{yze}t_{lyzw}$. In the rest of this section, we will numerically explore the impacts of the three parameters $a_2, \alpha,$ and β on the dynamics of (2.7) to observe biological implications.

4.1. impact of top predator z 's fear on its foraging for y via a_2

For this purpose, we set $\alpha = \beta = 0$ and observe how changes of a_2 will impact the dynamics of (2.7). To this end, we consider the following parameter values set:

$$b = 1.4, d = 0.4, d_1 = 0.4, d_2 = 0.01, a = 1, a_1 = 5.5, h_1 = 0.6, e_1 = 0.9, e_2 = 0.9, h_2 = 4. \tag{4.1}$$

With the above values, and by varying a_2 to four different values, we obtain numeric results shown in Fig. 5. Fig. 5(a) shows chaotic dynamics of the system (2.7) when $a_2 = 0.5$ ($a_2 = \gamma\alpha_{zsy}, \gamma = 1$), and the trajectories of this chaotic dynamics can be observed in the phase space. Then from Fig. 5(b) in which $a_2 = 0.2$ ($\gamma = 2/5$) is used, we observe periodic oscillations. When a_2 is further decreased to $a_2 = 0.15$ ($\gamma = 3/10$), the model demonstrates convergence to the positive equilibrium, as

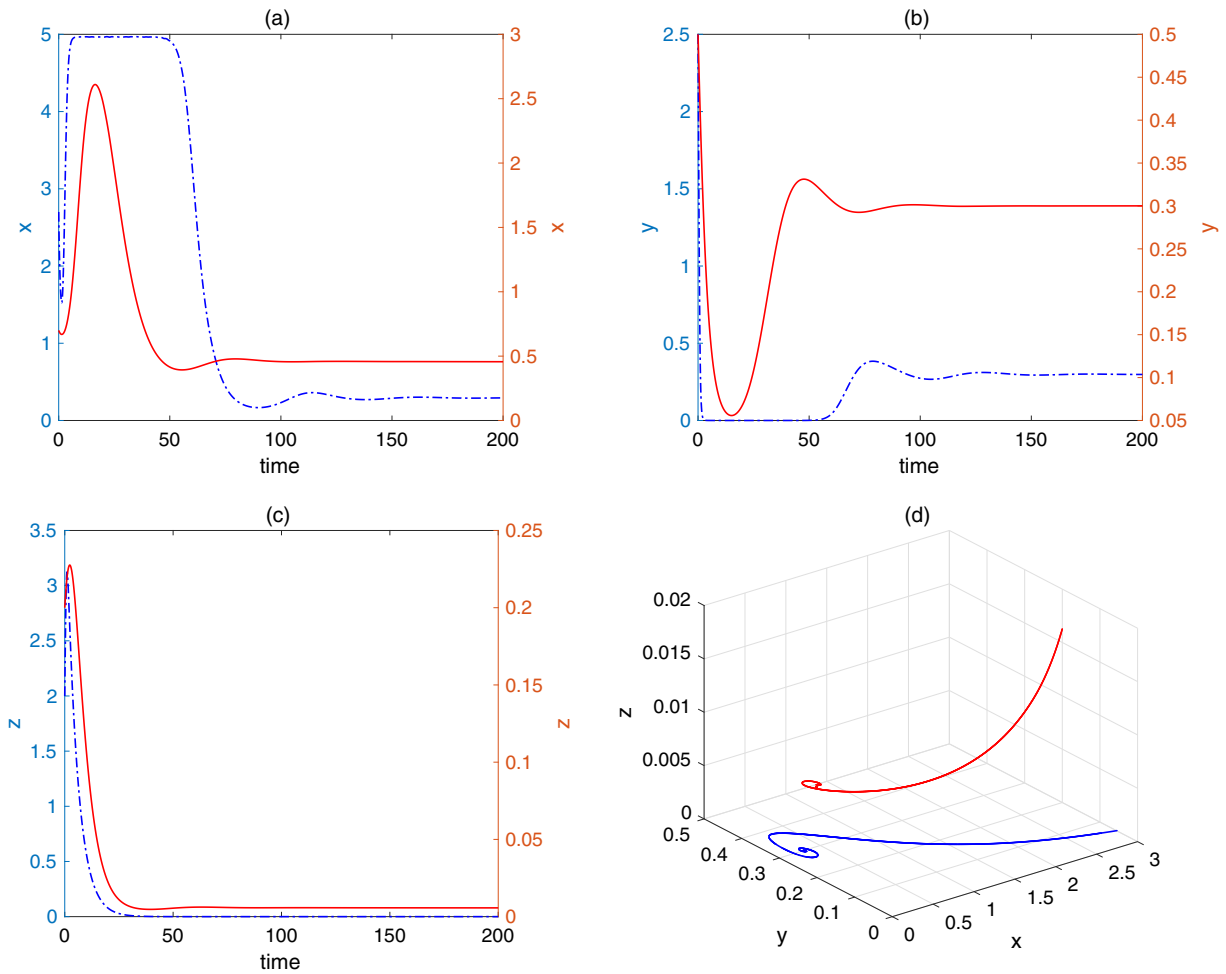


Fig. 4. System (2.7) allows a bistable scenario. The blue dot-dash line and red solid curve represent the solution starting at (2.7, 2.5, 2) and the solution starting at (0.7, 0.5, 0.2), respectively. They are attracted by two different equilibria ($b = 1.5, \alpha = 15.4, d = 0.01, a = 0.3, a_1 = 0.6, h_1 = 0.3, e_1 = 0.3, a_2 = 0.9, h_2 = 0.3, d_1 = 0.05, e_2 = 0.8, d_2 = 0.2, \beta = 73.9$). (For interpretation of the references to colour in this figure legend, the reader is referred to the web version of this article.)

is shown in Fig. 5(c). When $a_2 = 0.01$, γ is very small and the periodic oscillations appear again, $z(t)$ is driven to extinction (see Fig. 5(d)).

We can also demonstrate the effect of a_2 in the form of bifurcation diagram with respect to a_2 as in Fig. 6. From the diagrams, we see that there are four subintervals for a_2 : (i) if a_2 is sufficiently large, the system demonstrates chaotic dynamics. In this case, the interference ability of z is weaker than the interference from foraging activities of y . (ii) When a_2 is located in a medial range, the model produces the patterns of periodic dynamics. (iii) When a_2 is further reduced to a smaller medial range, the model supports the dynamics of convergence to the unique positive (co-existence) equilibrium. (iv) When a_2 is very small, the $x(t)$ and $y(t)$ resume periodic dynamics while $z(t)$ is driven to extinction.

4.2. impact of middle predator y 's fear on prey x 's birth rate via α

In their field study, Zanette et al. [40] have observed that the fear effect could affect reproduction even in the absence of direct killing. Such an effect is represented by the parameter α . To numerically explore the impact of α , we assume the top predator has no fear effect on the middle species' foraging for prey (i.e., $\beta = 0$). We adopt the values of parameters in (4.1) except changing $h_2 = 4$ to $h_2 = 16$ together with taking $a_2 = 0.15$. We then find that system can also exhibit chaotic dynamics as α varies. As shown in Fig. 7, the system has a chaotic attractor for $\alpha = 0.02$ (see Fig. 7(a)), a periodic attractor for $\alpha = 0.7$ (see Fig. 7(b)), and a unique stable interior equilibrium for $\alpha = 1$ (see Fig. 7(c)), respectively. The bifurcation diagrams in Fig. 8 with respect to the parameter α describe the switches between the above mentioned three types of dynamics for the system. As an additional way of judging chaotic dynamics, a variation of the maximum Lyapunov exponent for α is plotted in Fig. 9(a).

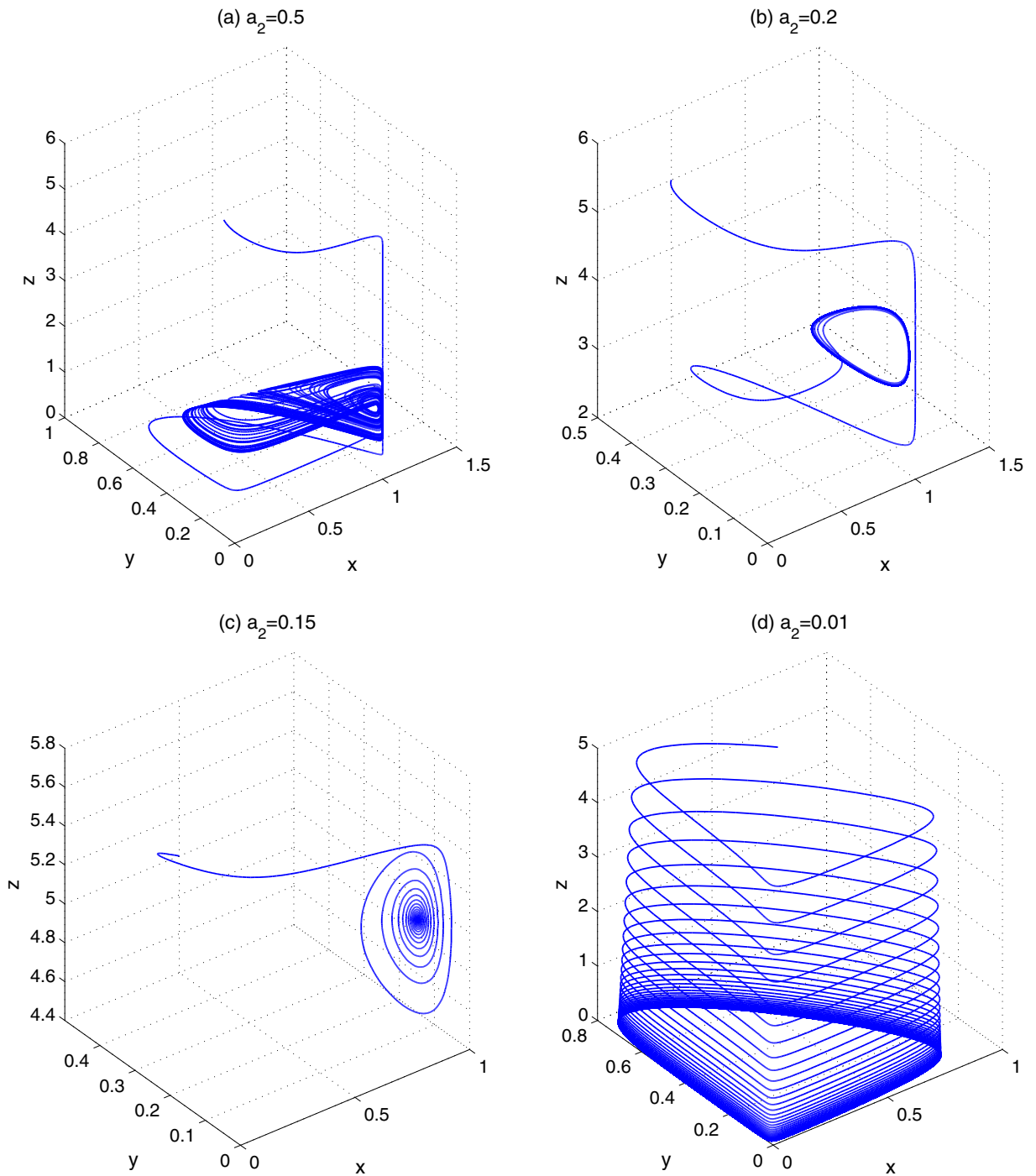


Fig. 5. Solutions of system (2.7) when $\alpha = 0 = \beta$ but with various values for a_2 . Other parameters are given in (4.1). (a) Chaotic dynamics when $a_2 = 0.5$; (b) periodic pattern when $a_2 = 0.2$; (c) stable focus when $a_2 = 0.15$; (d) periodic pattern when $a_2 = 0.01$ where $z(t)$ is driven to extinction.

The above simulations are done by fixing the other two parameters (a_2, β) at $(0.15, 0)$ and letting α vary. We point out that if (a_2, β) are fixed at different values, varying α may lead to different dynamics. To see this, we fix $\beta = 73.9$, $a_2 = 0.9$, and take α at three different values for $\alpha = 0$, $\alpha = 15.4$ and $\alpha = 20$. We observe that the longtime dynamics undergo changes from cyclic oscillation (see Fig. 10(a) when $\alpha = 0$) to a bistable scenario (see Fig. 10(b) when $\alpha = 15.4$), and to a stable focus (see Fig. 10(c) when $\alpha = 20$).

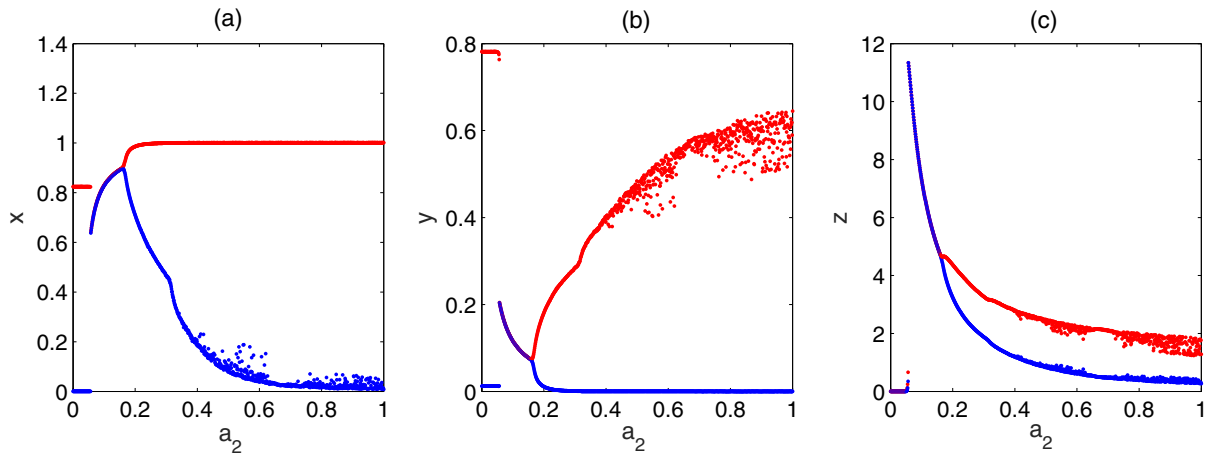


Fig. 6. Bifurcation diagram of the system (2.7) with respect to the parameter a_2 . Values of other parameters are the same as those in Fig. 5, given in (4.1).

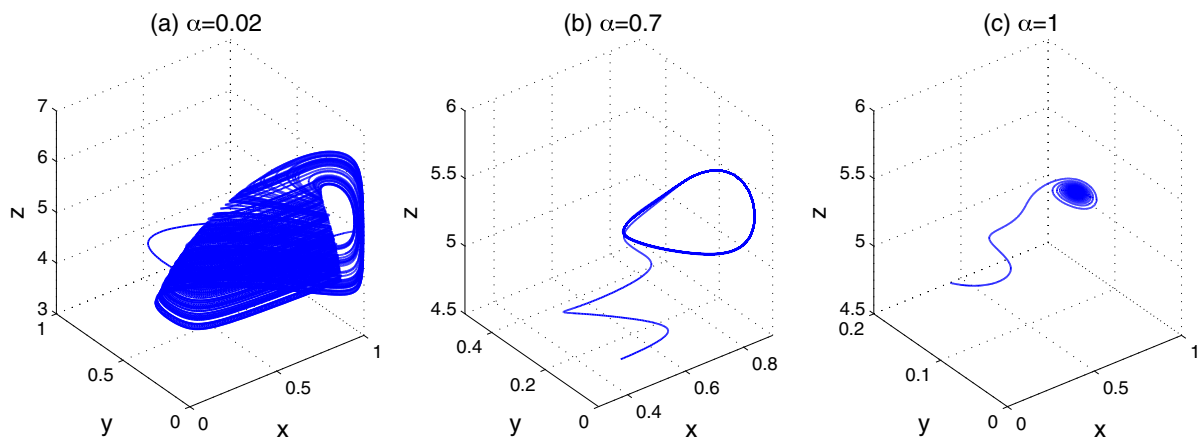


Fig. 7. Phase plot of system (2.7). (a) Chaotic dynamics; (b) periodic pattern; (c) stable focus. Here $a_2 = 0.15$, $\beta = 0$, $h_2 = 16$, other parameters are setting as (4.1).

4.3. impact of top predator z's fear on middle predator y's foraging for x via β

Next, we consider the effect of the top predator on the middle predator. To this end, we assume there is no fear effect of the middle predator on the bottom prey ($\alpha = 0$), but let β vary. As for the case of varying α in the above subsection, adopting the same parameter values in (4.1) except changing $h_2 = 4$ to $h_2 = 16$ together with taking $a_2 = 0.15$, we observe three different types of long time dynamics, as shown in Fig. 11: chaotic dynamics for $\beta = 0.01$ (see Fig. 11(a)), convergence to a periodic attractor for $\beta = 2$ (see Fig. 11(b)), and convergence to a positive equilibrium for $\beta = 8$ (see Fig. 11(c)), respectively. Bifurcation diagrams with respect to the parameter β are given in Fig. 12. And a variation of the maximum Lyapunov exponent for β is plotted in Fig. 9 (b).

In the above three subsections, among the three parameters a_2 , α and β that represent the fear effect at differential level, we numerically explored the impact of each of them by fixing the other two. We may also explore the joint effect of two of the three to have a better overview. For example, let us only fix $a_2 = 0.15$ and numerically explore the joint impact of α and β in the form of two-parameter bifurcations. Using the same set of parameter values as in (4.1) except changing $h_2 = 4$ to $h_2 = 16$, the bifurcation surfaces with respect to the parameters α and β are plotted in Fig. 13, respectively for x , y and z variables.

In addition, in order to more clearly express the impact of the introduction of the fear in the food chain, we consider the sign of the largest Lyapunov exponent in two-dimensional parameter space with varying two parameters α and β . Lyapunov diagrams for the $\alpha - \beta$ plane for the largest Lyapunov exponent are given in Fig. 14. The different color regions correspond to different dynamical behavior, the occurrence of chaotic dynamics is given by positive Lyapunov exponent and corresponds to blue regions; and green, yellow and red regions correspond to stable state and periodic orbits.

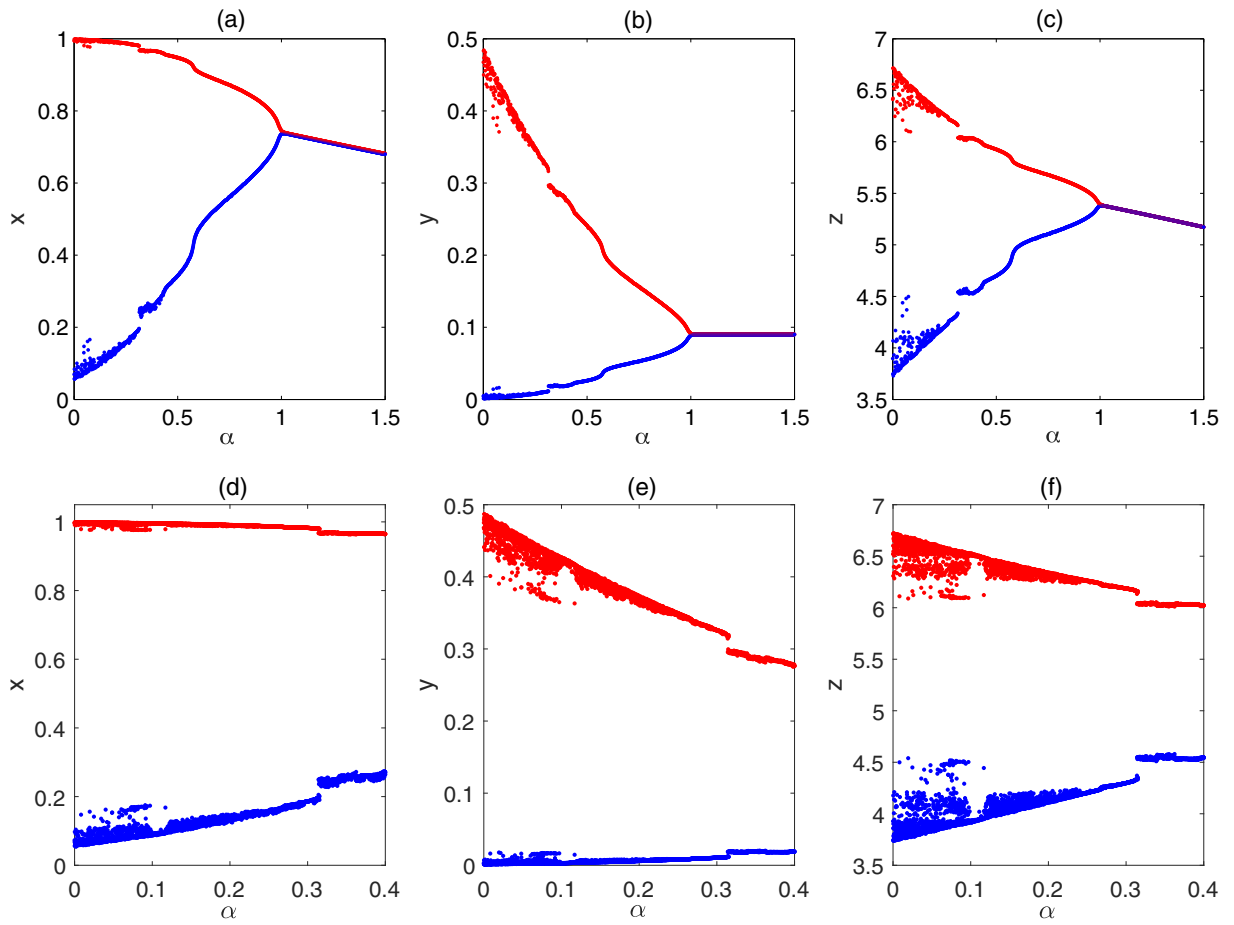


Fig. 8. Bifurcation diagram of the system (2.7) with respect to the bifurcation parameter α . Parameters are the same as those in Fig. 7, that is, they are given in (4.1). (d)-(e)-(f) are enlargements of (a)-(b)-(c) for small values of α corresponding to the chaotic dynamics in Fig. 7-(a).

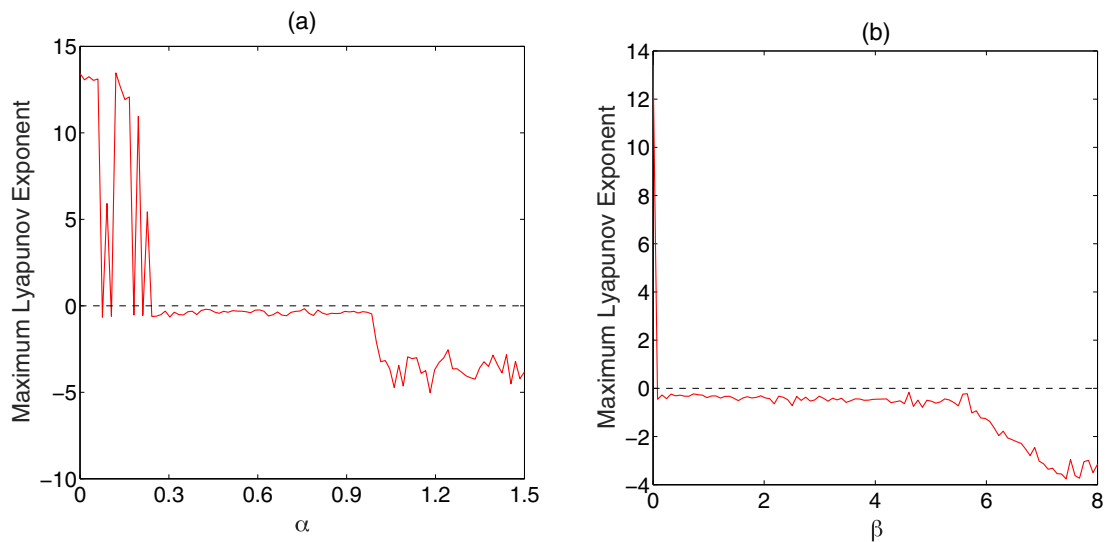


Fig. 9. A variation of the maximum Lyapunov exponent for α and β , respectively. Here (a) $\beta = 0$, (b) $\alpha = 0$, and other parameters are the same as (4.1).

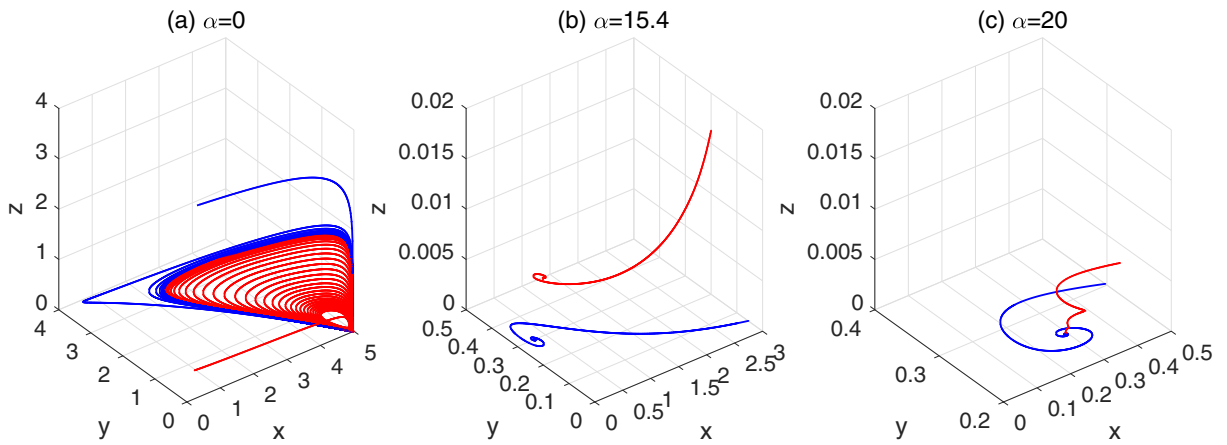


Fig. 10. A different bifurcation path including bistable equilibria when both a_2 and β are fixed at non-zero values. (a) The prey x , the middle predator y and the top predator z coexist cyclically where $\alpha = 0$; (b) system (2.7) allows a bistable scenario where $\alpha = 15.4$; (c) when $\alpha = 20$, all three species can coexist at an equilibrium. Other parameters are the same as those in Fig. 4.

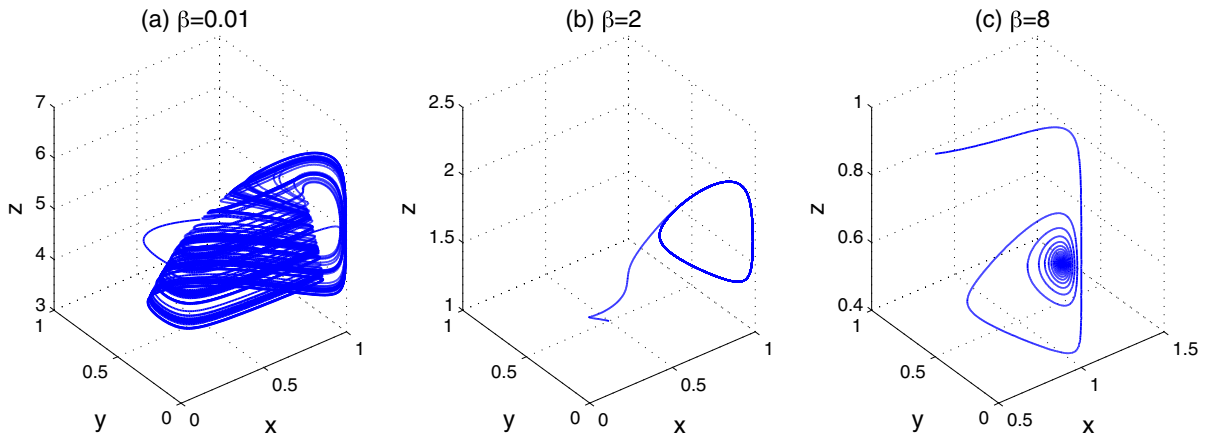


Fig. 11. Phase plot of system (2.7). (a) Chaotic dynamics; (b) periodic pattern; and (c) stable focus. Here $a_2 = 0.15, \alpha = 0, h_2 = 16$, other parameters are setting as (4.1).

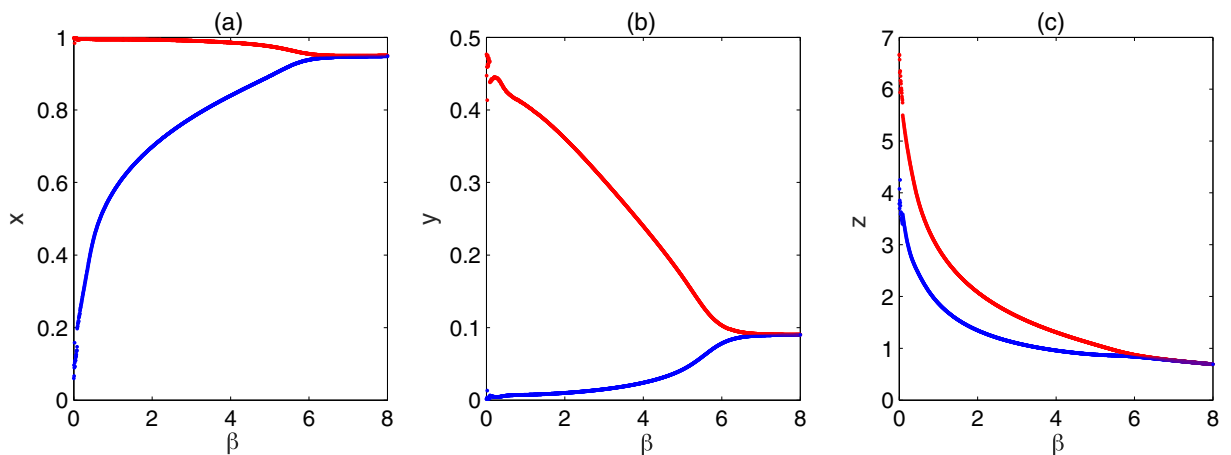


Fig. 12. The bifurcation diagram of the system (2.7) with respect to the bifurcating parameter β , parameters are the same as those in Fig. 11.

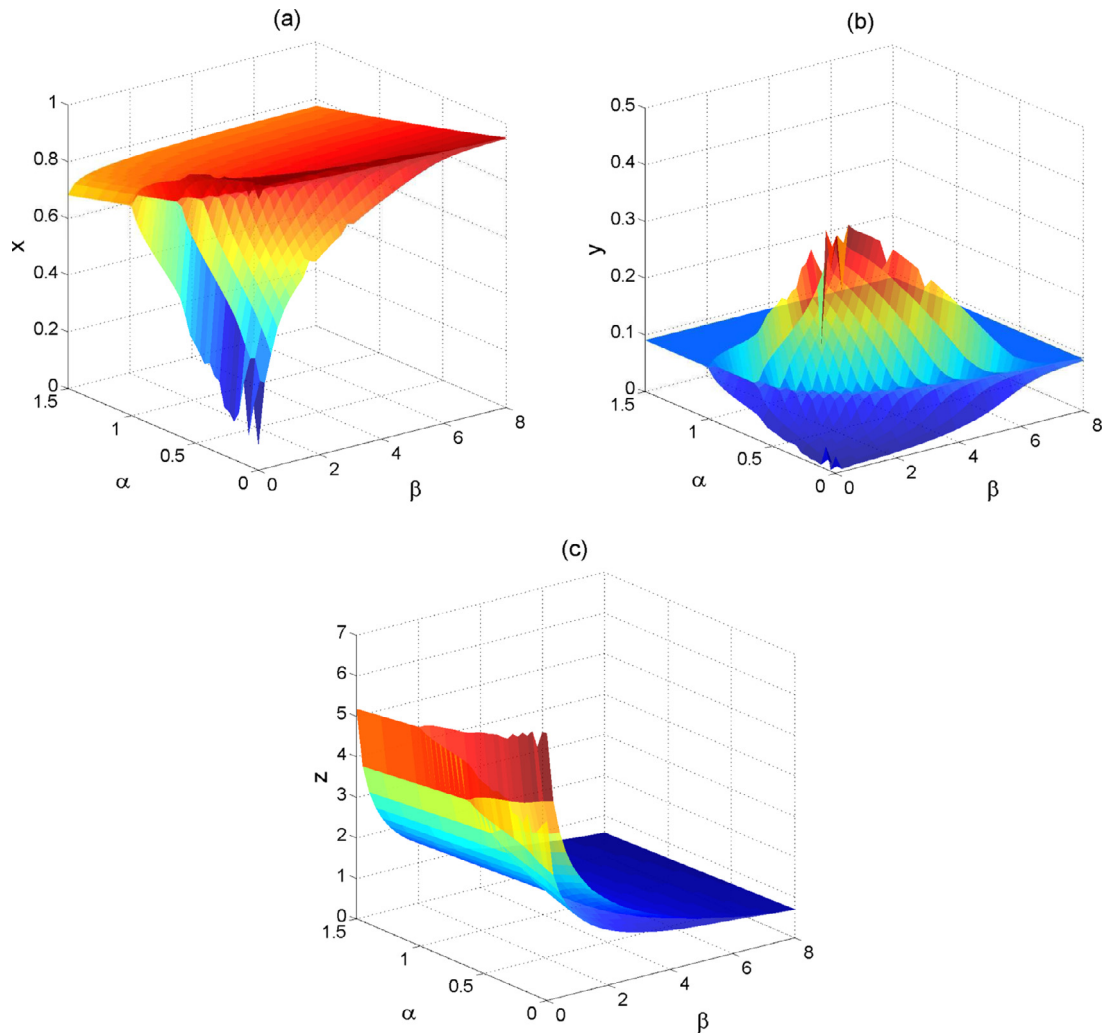


Fig. 13. Bifurcation surfaces for the prey x , the middle predator y and the top predator z , respectively, the bifurcation parameters are α and β . Here $a_2 = 0.15$, $h_2 = 16$, other parameters are setting as (4.1).

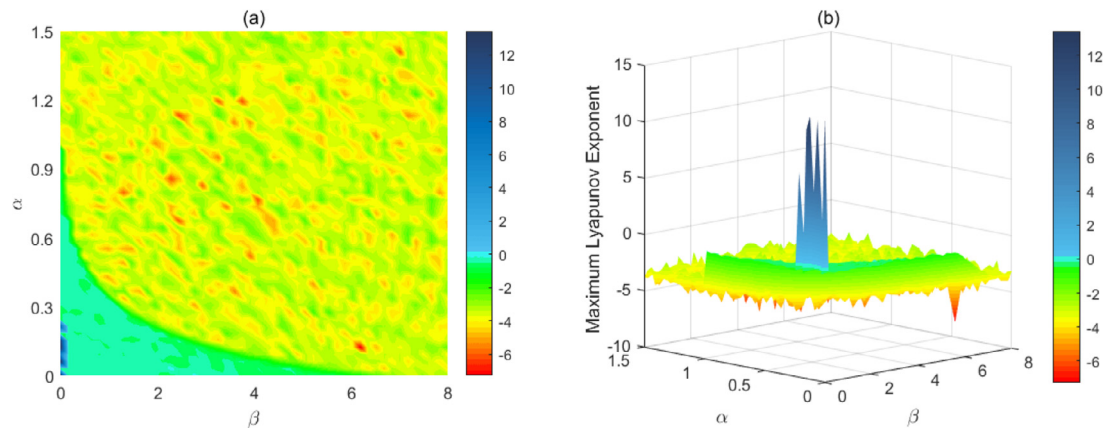


Fig. 14. Lyapunov diagrams for the $\alpha - \beta$ plane for the largest Lyapunov exponents. In blue the positive Lyapunov exponents indicate chaotic dynamics. Stable state and periodic orbits dynamics correspond to green, yellow and red regions. Here $a_2 = 0.15$, $h_2 = 16$, other parameters are setting as (4.1). (For interpretation of the references to colour in this figure legend, the reader is referred to the web version of this article.)

5. Conclusions and discussions

We have proposed a 3-D ODE model and rescaled system (2.6) to system (2.7), for a food chain ecosystem of three species, incorporated with the fear of the middle predator y on the bottom prey x , and the fear of the top predator z on the meso-prey y . These fear effects are reflected by three parameters: α accounts for the response of species x to the fear of species y , leading to a reduced production for species x ; β and a_2 account for the responses of species y to the fear of species z , leading a reduced foraging for species x and a reduced predation by species z .

We have theoretically analyzed the dynamics of the model (2.7) to obtain results about the longtime dynamics of (2.7). These results are described in terms of the model parameters, and hence, they can shed some lights on how the fear effects will affect the outcome of the interactions in the food chain system. Particularly, we have also numerically explored the impacts of the three parameters a_2 , α and β , and presented the results in the form of figures which are more visual and convenient for general readers. Our results show that, depending on the ranges of parameters, this system can have very rich dynamics including convergence to a unique co-existence equilibrium, bistability, sustained oscillations (or periodic behaviour), and even chaotic behaviour.

In particular, our numerical exploration on the impacts of the three fear related parameters has led to some interesting and meaningful observations, clearly showing how the fear effect in each related channel affects the longtime dynamics. For example, in the case $\beta = 0$ and $a_2 = 0.15$, we can see from Figs. 7 and 8 that when the fear level α is increased, the system experiences a bifurcation path of *chaotic* \rightarrow *periodic* \rightarrow *equilibrium*. So, large α will stabilize the system to a coexistence equilibrium. Such a phenomenon is also observed in [32] for the predator-prey model. But since the model in [32] is 2-D, there cannot be a chaotic behaviour for any range of parameters. Also, in the range of α supporting convergence to a coexistence equilibrium, as α increases, the densities of x and z decrease while the density of y increases. Such a phenomenon of *trophic cascade* is similar to the one experimentally reported in [30] and mathematically predicted in [36], but is caused by different factors: the trophic cascade is caused by the middle predator's fear on the bottom species, while in [30,36], the trophic cascade is caused by the top predator's fear on meso-species.

Note that the way the other fear parameter β is involved unique and novel: it is associated with the z variable governed by the third equation in the model but it occurs in both the first and the second equations. Its impact is also interesting. For example, for the case $\alpha = 0$ and $a_2 = 0.15$, from Fig. 11 and Fig. 12, we can see that, when β is increased (foraging of y for x is reduced), the system qualitatively experiences the same bifurcation path (surprisingly) as described in the preceding paragraph for increasing α : *chaotic* \rightarrow *periodic* \rightarrow *equilibrium*. However, quantitatively the densities of x and y increase and the density of z decreases as β increases, differing from trophic cascade observed in the preceding paragraph. These observations show that the roles of the two fear parameters α and β can be different.

We have also observed that when both cost and benefit of the fear effect on the three species are considered, the system (2.7) may allow a bistable scenario within a certain range of the parameters, as shown in Fig. 4. In such a scenario, there is the issue of the basin of attraction for each stable equilibrium, which is important as it determines the final destination of a solution by the initial value. Unfortunately, this is very challenging mathematically. We point out that a bistability scenario is also observed in [32] for the 2-D predator-prey system, but that bistability is for a stable equilibrium and a stable periodic solution, while the bistability observed here is for two stable equilibria.

The rich dynamics revealed from the system (2.7) can have some biological/ecological implications in biological control and biodiversity. Indeed, depending on the specific species in the food chain, one may have different goals/desires for these species on their extinction or persistence, and in the case of persistence, on their levels of densities. These goals may be achieved by creating some situations that can mimic some characteristics (e.g., vocal and visual) of the predators involved in the food chain, by which, the related fear effect(s) can be enhanced, helping to reach the desired longtime outcomes. Therefore, our results on the fear effect can help to maintain ecological balance and can be applied in ecological conservation efforts. We point out that our model is not specific to any particular three species forming a food chain, and thus, is of universality. However, we admit that, this study is mainly mechanistic, aiming to understand the mechanism of propagation of fear effect in a food chain. In general, activating a model with fear effect remains a challenge because in general it is not easy (if not impossible) to quantify the parameter(s) representing the fear effect.

We remark that, as far as we know, in the existing predator-prey models with fear effect, the fear effects are incorporated *intuitively*. In this paper, the fear parameter β is incorporated by a *rigorous derivation* by using the Holling's handling time argument, leading to the functional response $a_1x/(1 + a_1h_1x + \beta z)$ in the species y 's predation term. We believe this provides a new and reliable approach for incorporating fear effects to various predator-prey models. Recall that the well-known Beddington-DeAngelis functional response for the species y 's predation is of the form $ax/(1 + ahx + cy)$. Comparing our derived functional response $a_1x/(1 + a_1h_1x + \beta z)$ with the Beddington-DeAngelis functional response, one finds that the term $1 + ahx + cy$ in the denominator is replaced by $1 + a_1h_1x + \beta z$. This is because in our derivation, we have only considered the time wasted by each middle predator due to the interference by the top predator (hence βz) caused by the fear effect, but we have ignored the time wasted by each middle predator due to the interference caused by intra-species competition (hence cy). The predator-prey system with Beddington-DeAngelis functional response [2,7] has been considered in many papers, see, e.g., [9,16,17,22,41]. Thus, it is interesting and worthwhile to explore the situation with interferences from both fear effect and intra-species competition for the middle species y . This should lead to a functional response of the form $ax/(1 + ahx + cy + \beta z)$, which is expected to generate more complicated population dynamics. We leave this as a future research project.

Declaration of Competing Interest

The authors declare that they have no known competing financial interests or personal relationships that could have appeared to influence the work reported in this paper.

CRedit authorship contribution statement

Pingping Cong: Conceptualization, Methodology, Software, Writing - original draft. **Meng Fan:** Conceptualization, Methodology, Writing - review & editing. **Xingfu Zou:** Methodology, Writing - original draft, Writing - review & editing.

Acknowledgements

Cong is supported by the Short-term Study Abroad Program for PhD Students at NENU; Fan is supported by NSFC (No.12071068, 11671072); Zou is Supported by NSERC of Canada (RGPIN-2016-04665). This work is done when Pingping Cong is visiting Department of Applied Mathematics at University of Western Ontario. She would like to thank Dr Zou's research group for the enlightening discussion.

References

- [1] Altendorf KB, Laundré JW, Brown JS, González CAL. Assessing effects of predation risk on foraging behavior of mule deer. *J Mammal* 2001;82(2):430–9.
- [2] Beddington JR. Mutual interference between parasites or predators and its effect on searching efficiency. *J Anim Ecol* 1975;44:331–40.
- [3] Chen S, Liu Z, Shi J. Nonexistence of nonconstant positive steady states of a diffusive predator-prey model with fear effect. *J Nonlinear Model Anal* 2019;1:47–56.
- [4] Creel S, Christianson D, Liley S, Winnie JA Jr. Predation risk affects reproductive physiology and demography of elk. *Science* 2007;315:960–960.
- [5] Creel S, Christianson D. Relationships between direct predation and risk effects. *Trends Ecol Evol* 2008;23(4):194–201.
- [6] Das A, Samanta GP. Modeling the fear effect on a stochastic prey-predator system with additional food for the predator. *J Phys A-Math Theor* 2018;51(46):26. 465601
- [7] DeAngelis DL, Goldstein RA, O'Neill RV. A model for trophic interactions. *Ecology* 1975;56:881–92.
- [8] Duan D, Niu B, Wei J. Hopf-hopf bifurcation and chaotic attractors in a delayed diffusive predator-prey model with fear effect. *Chaos Solitons Fractals* 2019;123:206–16.
- [9] Fan M, Kuang Y. Dynamics of a nonautonomous predator-prey system with the beddington-deangelis functional response. *J Math Anal Appl* 2004;295(1):15–39.
- [10] Fan M, Kuang Y, Feng Z. Cats protecting birds revisited. *Bull Math Biol* 2005;67(5):1081–106.
- [11] Fan S. A new extracting formula and a new distinguishing means on the one variable cubic equation. *Nat Sci J Hainan Teach Coll* 1989;2(2):91–8.
- [12] Holling CS. Some characteristics of simple types of predation and parasitism. *Can Entomol* 1959;91(7):385–98.
- [13] Hua F, Sieving KE, Fletcher RJ, Wright CA. Increased perception of predation risk to adults and offspring alters avian reproductive strategy and performance. *Behav Ecol* 2014;25(3):509–19.
- [14] Kundu K, Pal S, Samanta S, Sen A, Pal N. Impact of fear effect in a discrete-time predator-prey system. *Bull Calcutta Math Soc* 2018;110:245–64.
- [15] Kumar V, Kumari N. Controlling chaos in three species food chain model with fear effect. *AIMS Mathematics* 2020;5(2):828–42.
- [16] Hwang TW. Global analysis of the predator-prey system with beddington-deangelis functional response. *J Math Anal Appl* 2003;281(1):395–401.
- [17] Hwang TW. Uniqueness of limit cycles of the predator-prey system with beddington-deangelis functional response. *J Math Anal Appl* 2004;290(1):113–22.
- [18] LaSalle JP. The stability of dynamical systems. Philadelphia: SIAM; 1976.
- [19] Lima SL, Dill LM. Behavioral decisions made under the risk of predation: a review and prospectus. *Can J Zool* 1990;68(4):619–40.
- [20] Mischaikow K, Smith H, Thieme HR. Asymptotically autonomous semiflows: chain recurrence and lyapunov functions. *Trans Am Math Soc* 1995;347(5):1669–85.
- [21] Mondal S, Maiti A, Samanta GP. Effects of fear and additional food in a delayed predator-prey model. *Biophys Rev Lett* 2018;13(04):157–77.
- [22] Naji RK, Balasim AT. Dynamical behavior of a three species food chain model with beddington-deangelis functional response. *Chaos Solitons Fractals* 2007;32(5):1853–66.
- [23] Panday P, Pal N, Samanta S, Chattopadhyay J. Stability and bifurcation analysis of a three-species food chain model with fear. *Int J Bifurcation Chaos* 2018;28(01):1850009.
- [24] Panday P, Pal N, Samanta S, Chattopadhyay J. A three species food chain model with fear induced trophic cascade. *Int J Appl Comput Math* 2019;5(4):100.
- [25] Preisser EL, Bolnick DI, Benard MF. Scared to death? the effects of intimidation and consumption in predator-prey interactions. *Ecology* 2005;86(2):501–9.
- [26] Ripple WJ, Beschta RL. Wolves and the ecology of fear: can predation risk structure ecosystems? *Bioscience* 2004;54(8):755–66.
- [27] Ronkainen H, Ylönen H. Behaviour of cyclic bank voles under risk of mustelid predation: do females avoid copulations? *Oecologia* 1994;97(3):377–81.
- [28] Sasmal SK. Population dynamics with multiple allee effects induced by fear factors—a mathematical study on prey-predator interactions. *Appl Math Model* 2018;64:1–14.
- [29] Sasmal SK, Takeuchi Y. Dynamics of a predator-prey system with fear and group defense. *J Math Anal Appl* 2020;481(1):123471.
- [30] Suraci JP, Clinchy M, Dill LM, Roberts D, Zanette LY. Fear of large carnivores causes a trophic cascade. *Nat Commun* 2016;7:10698.
- [31] Upadhyay RK, Mishra S. Population dynamic consequences of fearful prey in a spatiotemporal predator-prey system. *Math Biosci Eng* 2019;16(1):338–72.
- [32] Wang X, Zanette L, Zou X. Modelling the fear effect in predator-prey interactions. *J Math Biol* 2016;73:1179–204.
- [33] Wang X, Zou X. Modeling the fear effect in predator-prey interactions with adaptive avoidance of predators. *Bull Math Biol* 2017;79(6):1325–59.
- [34] Wang X, Zou X. Pattern formation of a predator-prey model with the cost of anti-predator behaviors. *Math Biosci Eng* 2018;15(3):775–805.
- [35] Wang Y, Zou X. On a predator-prey system with digestion delay and anti-predation strategy. *J Nonlinear Sci* 2020;30:1579–605.
- [36] Wang Y, Zou X. On mechanisms of trophic cascade caused by anti-predation response in food chain. *Math Appl Sci Eng* 2020;1:181–206.
- [37] Ylönen H. Weasels *Mustela nivalis* suppress reproduction in cyclic bank voles *Clethrionomys glareolus*. *Oikos* 1989;55(1):138–40.
- [38] Ylönen H, Ronkainen H. Breeding suppression in the bank vole as antipredatory adaptation in a predictable environment. *Evol Ecol* 1994;8(6):658–66.
- [39] Ylönen H. Vole cycles and antipredatory behaviour. *Trends Ecol Evol* 1994;9(11):426–30.
- [40] Zanette LY, White AF, Allen MC, Clinchy M. Perceived predation risk reduces the number of offspring songbirds produce per year. *Science* 2011;334(6061):1398–401.
- [41] Zhao M, Lv S. Chaos in a three-species food chain model with a beddington-deangelis functional response. *Chaos Solitons Fractals* 2009;40(5):2305–16.
- [42] Zhang J, Fan M, Kuang Y. Rabbits killing birds revisited. *Math Biosci* 2006;203(1):100–23.